

Received November 16, 2020, accepted December 9, 2020, date of publication December 14, 2020, date of current version December 23, 2020.

Digital Object Identifier 10.1109/ACCESS.2020.3044529

# Load Balancing Scheme in Hybrid WiGig/LiFi Network

**MOHAMMED FARRAG**<sup>1,2</sup>, (Member, IEEE),  
**MOHAMMED ZUBAIR SHAMIM**<sup>1,3</sup>, (Senior Member, IEEE),  
**MOHAMMED USMAN**<sup>1</sup>, (Senior Member, IEEE), AND  
**HANY S. HUSSEIN**<sup>1,4</sup>, (Senior Member, IEEE)

<sup>1</sup>Department of Electrical Engineering, King Khalid University (KKU), Abha 62529, Saudi Arabia

<sup>2</sup>Electrical Engineering Department, Assiut University, Assyt 71515, Egypt

<sup>3</sup>Center for Artificial Intelligence, King Khalid University, Abha 61413, Saudi Arabia

<sup>4</sup>Electrical Engineering Department, Aswan University, Aswan 81528, Egypt

Corresponding author: Hany S. Hussein (hahussein@kku.edu.sa)


This work was supported by the Deanship of Scientific Research, King Khalid University, Abha, Saudi Arabia, through the Research Groups Program, under Grant R.G.P.1/202/41.

**ABSTRACT** Recently, Light fidelity (LiFi) is proposed as a high-speed wireless communication technology. A LiFi access point provides the service in an area of a few square meters known as LiFi attocells. Therefore, by utilizing frequency reuse, LiFi networks provide a high spatial spectral efficiency. Unfortunately, beside to uplink and mobility problems, the LiFi networks suffer more difficulties with increasing of the number of mobile devices. As a solution, hybrid LiFi and radio frequency (RF) networks are proposed. In this article, a hybrid network, that combines LiFi with RF Wireless Gigabit Alliance (WiGig) networks, is proposed. The WiGig access points will provide gigabit-per-second data rates as a result of the availability of large bandwidth at the millimeter wave (mmWave) frequency ranges. Such hybrid networks need an efficient load balancing (LB) scheme. In this article, two modified versions of the separate optimization algorithm (SOA) are proposed; Assign WiGig First SOA (AWFS) algorithm and Consecutive Assign WiGig First SOA (CAWFS) algorithm. The simulation results show that the two proposed algorithms offer better achievable data rates and outage probability performances compared with the SOA algorithm.

**INDEX TERMS** Hybrid network, LiFi communications, mmWave, WiGig network.

## I. INTRODUCTION

The expanding number of portable devices with multi-media and data-demanding applications, considering the restricted accessibility of the radio frequency (RF) range, implies that current mobile systems are at their most extreme capacity. Light fidelity (LiFi) innovation, which utilizes 300 THz free-licensed and unoccupied optical range, has a considerable interest as a solution to the spectrum shortage problem [1]–[4]. Using LiFi technology, a full small-cell wireless network that including multi-user, bi-directional and multiple access communication can be defined. LiFi access point (AP) covers a few square meters known as LiFi attocells. Small attocells protect users from receiving severe interference from nearby LiFi APs. So, by utilizing frequency reuse,

The associate editor coordinating the review of this manuscript and approving it for publication was Amjad Mehmood .

LiFi networks provide a high spatial spectral efficiency (SE). Unfortunately, beside to uplink and mobility problems, the LiFi networks suffer difficulties with increasing of the number of mobile devices. To solve these problems and to provide an acceptable level of quality of service (QoS), a hybrid LiFi/RF network was proposed [5], [6] and [7].

In the same time, Wireless Gigabit Alliance (WiGig) provided WiFi protocol with the huge transmission capacities using the millimetre wave (mmWave) band make it a promising candidate to solve the spectrum shortage problem as a RF communication framework [8]. WiGig signal cannot break through walls, instead of that, it reflects from walls, ceilings, floors and objects. WiGig has the ability to track users via beam steering mechanism getting it applicable for user mobility scenarios. So, WiGig is suited either for stationary or mobile users. Unfortunately, if the number of users, that are served by the WiGig AP, is increased upon a certain value,

side-lobe levels is increased which cause inter-beam interference (IBI). The simulation results in [9] showed that, with increasing of the number of users, the hybrid beamforming performance in IEEE 802.11ad increases and then decreases. Moreover, in [10] it is proved that the number of users is linearly proportional with the beamforming overhead, and inversely proportional with the system throughput. In [11], it is shown that with increasing of the number of users, the time-elapsed and system complexity are increased and the throughput gain is decreased. Therefore, it is recommended for the WiGig network to support only a finite number of users. The optimum number of users which maximizes the SE is provided in [12].

Working in totally different electromagnetic ranges prevent LiFi and WiGig applications from causing interference to each other [6]. This motivates the creation of hybrid system that combines both LiFi with WiGig frameworks. On one hand, WiGig can attain a data rate of 7 Gb/s [5]. On the other hand, a single light emitting diode (LED) can achieve data rate of more than 3 Gb/s [7]. Since LiFi does not affect WiGig range and throughput, the overall throughput of a LiFi/WiGig hybrid network is always more than that of stand alone WiGig or LiFi system [6].

In this article, we propose an ultra-high capacity indoor WLAN network based on integrating between the LiFi, using the visible light band, and the WiGig, using the mmWave band, instead of traditional WiFi. In the previous hybrid LiFi/RF network, the WiFi network provides the desired QoS to the users with low-level optical signals [5], [6] and [7]. In the proposed work, and because of the WiGig limited number of users, only the  $N_{max}$  users with minimum LiFi data rate are assigned to the WiGig AP, while the others will be assigned to the LiFi APs. To design the LiFi/WiGig WLAN, efficient algorithms for LiFi/WiGig vertical handover should be addressed. In the hybrid network, each user should be assigned to only one AP, LiFi or WiGig. So, load balancing (LB) scheme should be utilized. Due to both the limited size of LiFi attocells and limited number of users in WiGig AP, fair and efficient LB in a hybrid LiFi/WiGig network can be a challenge. This work aims to develop LB scheme that guarantee high user throughput, fairness and stability. According to [13], system LB composed of two main processes; access point assignment (APA) and resource allocation (RA). In [14], [15], joint load balancing (LB) and power allocation (PA) algorithms for hybrid RF/VLC networks were proposed. An iterative algorithm was proposed to maximize the total system capacity and enhance the system fairness based on the exact or approximate interference information for all users. In [16], a dynamic cell formation method jointly with a load balancing strategy for hybrid VLC/RF networks was proposed. The centralized and decentralized load balancing algorithms taking into consideration the topology of the hybrid VLC/RF networks to manage the transmission resources. A comparison between many types of LB schemes like Optimization based scheme (OBS) as Joint optimization algorithm (JOA) and Separate optimization algorithm (SOA),

Fuzzy logic-based scheme (FBS) [17] and Evolutionary game theory-based scheme (EBS) [18] [19] is given in [20]. In [20] the simulation results show that beside the ability to approach global optimum, JOA outperforms SOA significantly in terms of user data rate. On the other hand, computational complexity of SOA is much lower than JOA. In this article, two modified versions of the SOA algorithms are proposed where only the  $N_{max}$  users with minimum LiFi data rate are chosen to be assigned to the WiGig AP, while the others will be assigned to the LiFi APs; each user will be assigned to the LiFi AP which will provide the maximum available data rate.

The rest of the paper is organised as follows: The hybrid system model, LiFi and WiGig channel models and review about the SOA algorithm is introduced in Section II. A detailed description of the proposed LB schemes are explained in Section III. The performance evaluation and throughput analysis are simulated and discussed in Section IV. Finally, the conclusions are drawn in Section V.

## II. SYSTEM MODEL AND SOA ALGORITHM

### A. SYSTEM SETUP

As shown in Fig. 1, the proposed system composed of only one WiGig AP and  $N_{LF}$  LiFi APs which are distributed on the ceil of the room. It is assumed that the set of  $N_{\mu}$  users, indicated as  $\mathcal{U} = \{\mu_i\}_{i=1}^{N_{\mu}}$ , is distributed over the room area. A central unit (CU) is connected using error free links to all APs. In the LiFi network, the AP is consisting of several light emitting diodes (LEDs), while the mobile receivers have perpendicular photo detectors (PDs). Therefore, the angles of irradiance and incidence are supposed to be equal. Based on the spectrum reuse between all LiFi APs, the LiFi system provides high spatial SE [21]. However, the users staying in the overlapping cell edges may have

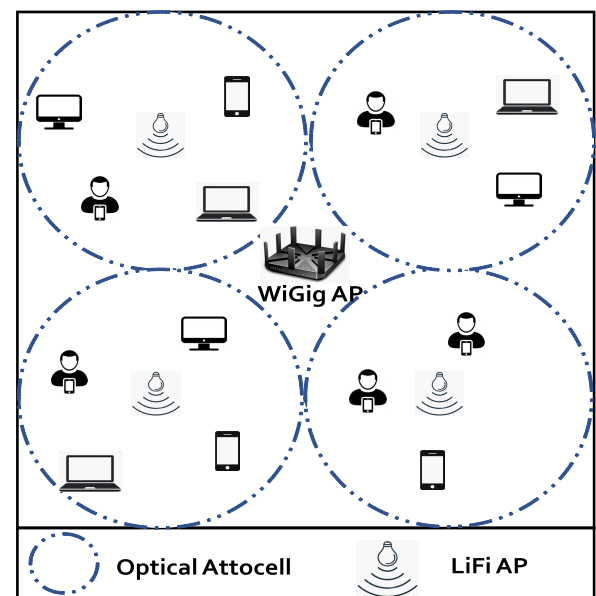


FIGURE 1. System model.

a heavy inter-carrier-interference (ICI) which significantly degrades the user data rate [6], [22]. To solve this problem, the system is boosted by an WiGig AP. For downlink communications, each user is allocated to a LiFi AP or the WiGig AP. Therefore, the network load balancing (LB) scheme that addresses the tasks of access point assignment (APA) and time slot resource allocation (RA) is needed. In the dynamic indoor environments with varying channels CSI, APA and RA should be updated each a quasi-static state  $T_n$ , where  $n$  is the states sequence number [22].

In the considered system, the set of LiFi APs and the WiGig AP are denoted by  $\mathcal{C} = \{c|c \in [0, N_{LF}], c \in \mathbb{Z}\}$ , where  $(c = 0) \in \mathcal{C}_R$  refers to the WiGig AP and  $\mathcal{C}_l = \{c\}_1^{N_{LF}}$  refer to the LiFi APs and  $\mathbb{Z}$  is the set of integer numbers.

## B. THE MODEL OF THE LiFi CHANNEL

In indoor scenarios, the gain of the optical channel consists of two different components; the line of sight (LoS) and the reflection components. According to [23], the LoS component is represented as:

$$H_{\mu,\alpha} = \begin{cases} \frac{(m+1)A_p g(\theta) T_s(\theta)}{2\pi(z^2 + \omega^2)} \cos^m(\phi) \cos(\theta), & 0 \leq \theta \leq \Theta_F \\ 0, & \theta < \Theta_F \end{cases} \quad (1)$$

where  $m = -1/\log_2(\cos(\theta_{1/2}))$  is the Lambertian index with half-intensity radiation angle  $\theta_{1/2}$ ;  $A_p$  is the PD physical area;  $z$  is the horizontal distance from the optical receiver of the  $\mu^{th}$  user to the  $\alpha^{th}$  LiFi AP;  $\omega$  is the room height;  $\phi$  and  $\theta$  are the irradiation and incidence angles, respectively;  $\Theta_F$  is the half angle of field-of-view (FOV) of the receivers;  $T_s(\theta)$  is the optical filter gain; and the concentrator gain  $g(\theta)$  can be expressed as follows:

$$g(\theta) = \begin{cases} \frac{\chi^2}{\sin^2(\Theta_F)}, & 0 \leq \theta \leq \Theta_F \\ 0, & \theta < \Theta_F \end{cases} \quad (2)$$

where  $\chi$  is the refractive index.

According to [22], if the LiFi baseband modulation bandwidth  $B$  is less than 25 MHz, the reflection component could be neglected. Moreover, it was reported in [24], [25] that, more than 95% of the total energy collected by LiFi photo-detector in indoor scenarios produces from the direct or line-of-sight (LoS) component. Hence in this article the bandwidth  $B$  is assumed to be 20 MHz, the reflection component is not considered in the model of the LiFi channel. Based on [26], the intensity modulation (IM) baseband communication and direct detection (DD) are used in LiFi systems. The LiFi positive and real signals are transmitted in the optical power form. The conversion between the average electric power of signals  $P_{elec}$  and the average DC optical power  $P_{opt}$  is represented as [27]:

$$\iota = P_{opt} / \sqrt{P_{elec}} \quad (3)$$

The signal-to-interference-plus-noise ratio (SINR) at the user  $\mu$  which is allocated to  $\alpha$  AP is:

$$\text{SINR}_{\mu,\alpha} = \frac{(\kappa P_{opt} H_{\mu,\alpha})^2}{\iota^2 N_0 B + (\kappa P_{opt})^2 \sum H_{\mu,else}^2} \quad (4)$$

where  $\kappa$  is the optical to electric conversion efficiency at the receivers;  $N_0 [A^2/Hz]$  is the noise power spectral density;  $H_{\mu,\alpha}$  is the channel gain between the  $\mu^{th}$  user and the  $\alpha^{th}$  LiFi AP; and  $H_{\mu,else}$  is the channel gain between the  $\mu^{th}$  user and the interfering LiFi APs Eq. (1).

To calculate the achievable data rate between user  $\mu$  and LiFi AP  $\alpha$ , Shannon capacity is used. The achievable data rate is represented as follows:

$$R_{\mu,\alpha}^{(n)} = B \log_2(1 + \text{SINR}_{\mu,\alpha}^{(n)}), \quad (5)$$

## C. THE MODEL OF THE WiGig CHANNEL

Assume a WiGig wireless communication network with WiGig AP, with  $N_{BS}$  antennas and  $N_{RF}$  RF chains, communicates with  $N_\mu$  mobile users; each with  $N_{MS}$  antennas. Assume that the AP is connected with each user  $\mu$  through only one stream. Furthermore, the maximum number of simultaneously users served by the WiGig AP  $N_{max}$  is calculated depending on [12].

In the downlink, a  $U \times U$  baseband precoder  $F_{BB} = [f_1^{BB}, f_2^{BB}, \dots, f_U^{BB}]$  then an  $N_{BS} \times U$  RF precoder,  $F_{RF} = [f_1^{RF}, f_2^{RF}, \dots, f_U^{RF}]$ , are applied by the BS [28], where  $U$  is the number of mobile users. The transmitted signal can be expressed as;

$$x = F_{RF} F_{BB} s, \quad (6)$$

where the  $U \times 1$  transmitted symbols vector  $s = [s_1, s_2, \dots, s_U]^T$  with  $E[ss^*] = (P/U)I_U$ , and  $P$  is the average total transmitted power.

For simplicity, a narrowband block-fading channel model, [11], [12], [28]–[30], [31] and [32], is adopted where the received signal at the  $\mu^{th}$  user is;

$$r_\mu = H_\mu \sum_{n=1}^U F_{RF} f_n^{BB} s_n + n_\mu \quad (7)$$

where the  $N_{MS} \times N_{BS}$  matrix;  $H_\mu$  is the mmWave channel between the WiGig AP and the  $\mu^{th}$  user, and  $n_\mu \sim N(0, \sigma^2 I)$  is the Gaussian noise corrupting the received signal.

At the  $\mu^{th}$  user, the received signal  $r_\mu$  is addressed by the RF combiner  $w_\mu$ :

$$y_\mu = w_\mu^* H_\mu \sum_{n=1}^U F_{RF} f_n^{BB} s_n + w_\mu^* n_\mu \quad (8)$$

In [28], to integrate the expected limited scattering in the mmWave channel [33], a geometric channel model with  $L_u$  scatterers for the channel of user  $u$  was adopted. Each scatterer was assumed to represent a separate propagation path from the BS to the user  $u$ . The conventional approaches for scattering channel modelling represent one of the two extremes: idealized statistical models representing a

rich scattering environment [34] and parametrized physical models that describe realistic scattering environments via the angles and gains associated with different propagation paths [35]. In [36], the intermediate virtual channel representation that captures the essence of physical modelling without its complexity and provides a simple geometric interpretation of the scattering environment was proposed. Under this model, the channel  $H_\mu$  can be expressed as;

$$H_\mu = \sqrt{\frac{N_{BS}N_{MS}}{L_\mu}} \sum_{l=1}^{L_\mu} \rho_{\mu,l} a_{MS}(\theta_{\mu,l}) a_{BS}^*(\phi_{\mu,l}), \quad (9)$$

where  $\rho_{\mu,l}$  is  $l^{th}$  path complex gain, with  $\mathbb{E}[|\rho_{\mu,l}|^2] = \bar{\rho}$ . The  $l^{th}$  path's angles of arrival and departure (AoAs/AoDs) are  $\theta_{\mu,l}$  and  $\phi_{\mu,l} \in [0, 2\pi]$ , respectively. Finally,  $a_{MS}(\theta_{\mu,l})$  and  $a_{BS}^*(\phi_{\mu,l})$  are the antenna array response vectors of the AP and  $\mu^{th}$  user respectively. Then, the achievable rate of user  $\mu$  is

$$R_\mu = \log_2 \left( 1 + \frac{\frac{P}{U} |w_\mu^* H_\mu F_{RF} f_\mu^{BB}|^2}{\frac{P}{U} \sum_{n \neq \mu} |w_n^* H_n F_{RF} f_n^{BB}|^2 + \sigma^2} \right). \quad (10)$$

The sum-rate of the system is then:

$$R_{sum} = \sum_{\mu=1}^{N_{max}} R_\mu. \quad (11)$$

### D. SEPARATE OPTIMIZATION ALGORITHM (SOA)

According to [20], in SOA algorithm, APA and RA processes are sequentially optimized. Based on the high spatial SE of LiFi network, the APA is realized where users with LiFi data rates more than a certain threshold  $\gamma$ , will be assigned to LiFi APs and the others would be allocated to the RF APs. Furthermore, the maximal effective throughput criterion is applied. For each user  $\mu$  and given that

$$r_{\mu,c} = \begin{cases} R_{\mu,\alpha}, & c \in \mathcal{C}_L \quad \text{Eq. 5} \\ R_\mu, & c \in \mathcal{C}_R \quad \text{Eq. 10} \end{cases} \quad (12)$$

The chosen maximal link data rate LiFi AP is:

$$\tau_{1,\mu} = \arg \max_{j \in \mathcal{C}_L} r_{\mu,j}, \quad (13)$$

where  $r_{\mu,j}$  is the LiFi data rate. Under assumption of equally shared time resource by all users in the attocell, the potential data rate of each user is:

$$\lambda_\mu = r_{\mu,j} / M_{\tau_{1,\mu}} \quad (14)$$

where  $M_{\tau_{1,\mu}}$  is the number of users assigned to the LiFi AP  $\tau_{1,\mu}$ . The users with  $\lambda_\mu < \gamma$  will be assigned to RF APs based on the following criterion;

$$\tau_{2,\mu} = \arg \max_{j \in \mathcal{C}_R} r_{\mu,j}, \quad \lambda_\mu < \gamma. \quad (15)$$

According to Eqs. (13, 15), in SOA, the APA result is:

$$g_{\mu,\alpha}^{(SOA)} = \begin{cases} 1, & \alpha = \begin{cases} \tau_{1,\mu}, & \lambda_\mu \geq \gamma \\ \tau_{2,\mu}, & \lambda_\mu < \gamma \end{cases} \\ 0, & \text{Otherwise} \end{cases} \quad (16)$$

In the RA step, each AP allocates the time resources to the connected users independently. The generalized  $\beta$ -proportional fairness function  $\Psi_\beta(x)$ , that takes into account both user fairness and sum-rate [37] and can be formulated as a utility maximisation problem, where;

$$\Psi_\beta(x) = \begin{cases} \log(x), & \beta = 1 \\ \frac{x^{1-\beta}}{1-\beta}, & \beta \geq 0, \beta \neq 1 \end{cases} \quad (17)$$

where  $\beta$  is the fairness coefficient and  $x$  is the achievable data rate. After APA step, the RA step can be formulated as follows:

$$k_{\mu,\alpha}^{(SOA)} = \frac{r_{\mu,\alpha}^{\frac{1}{\beta}-1}}{\sum_{i \in \mathcal{U}_\alpha} r_{i,\alpha}^{\frac{1}{\beta}-1}} \quad (\beta > 0). \quad (18)$$

Algorithm 1 summarizes the SOA steps.

---

### Algorithm 1: SOA Algorithm

---

**Initialisation:**  $r_{\mu,\alpha}$  and  $\gamma$ ;  
**for** each user  $\mu_i$  where  $i = 1$  to  $N_\mu$  **do**  
    the CU calculates  $\tau_{1,\mu}$  and the optical data rate  $\lambda_\mu$   
    based on Eqs. (13, 14), respectively;  
    **if**  $\lambda_\mu \geq \gamma$  **then**  
        the user will assigned to LiFi AP  $\tau_{1,\mu}$ ;  
    **else**  
        the user will assigned to RF AP  $\tau_{2,\mu}$  using  
        Eq. (15);  
    **end**  
**end**  
In RA step, each AP determines the resource portion for its allocated users, using Eq. (18).

---

### III. PROPOSED LOAD BALANCING ALGORITHMS

In this article, we propose an ultra-high capacity indoor WLAN network based on integrating between the LiFi and the WiGig using the mmWave band instead of traditional WiFi. In the previous work, hybrid LiFi/RF network based on WiFi technology was proposed [5], [6] and [7]. In this work, we propose to use WiGig technology instead of WiFi. Due to the limited number of users could be simultaneously served by the WiGig AP [9]–[11], only the  $N_{max}$  users with minimum LiFi data rate are assigned to the WiGig AP, while the others will be assigned to the LiFi APs. To implement the LiFi/WiGig WLAN, efficient algorithms for LiFi/WiGig vertical handover should be addressed. For downlink communications in a hybrid network, each user can be served by only one AP; LiFi or WiGig, so LB should be addressed. In this work, two modified versions of SOA algorithm are proposed. In the proposed algorithms, the  $N_{max}$  users with minimum LiFi data rate is assigned to the WiGig AP, while the others will be assigned to the LiFi APs; each user will be assigned to the LiFi AP which will provide the maximum available date rate.



### A. ASSIGN WiGig FIRST SOA (AWFS) LB ALGORITHM

In the assign WiGig first SOA (AWFS) LB algorithm, a set  $\mathcal{C}_R$  contains the  $N_{max}$  users with minimum LiFi rates is constructed. Then, all users belong to the set  $\mathcal{C}_R$  will be assigned to the the WiGig AP, while other users will assigned to the LiFi AP. The proposed APA of the AWFS algorithm is expressed as follows:

$$g_{\mu,\alpha}^{(AWFS)} = \begin{cases} 1, & \alpha = \begin{cases} \tau_{1,\mu}, & \mu \notin \mathcal{C}_R \\ \text{WiGig AP}, & \mu \in \mathcal{C}_R \end{cases} \\ 0, & \text{Otherwise} \end{cases} \quad (19)$$

---

#### Algorithm 2: AWFS Algorithm

---

**Initialisation:**  $r_{\mu,\alpha}$  and  $\gamma$ ;

For all users,  $\tau_{1,\mu}$  and  $\lambda_\mu$  are calculated based on Eqs. (13, 14), respectively;

Construct the vector  $R = \{\lambda_\mu\}_{\mu=1}^{\mathcal{U}}$ ; where users are arranged ascendantly according to data rate, and the indices of the  $N_{max}$  users with the lowest data rates are added to the vector  $I_m$ .

**for** each user  $\mu_i$  where  $i = 1$  to  $N_\mu$  **do**

**if**  $i \in I_m$  **then**

        the user will assigned to the WiGig AP;

**else**

        the user will assigned to LiFi AP  $\tau_{1,\mu}$ ;

**end**

**end**

---

### B. CONSECUTIVE ASSIGN WiGig FIRST SOA (CAWFS) LB ALGORITHM

Due to the random distribution of the mobile users, some LiFi APs may be crowded by mobile users i.e. the number of users assigned to a certain LiFi AP  $M_{\tau_{1,\mu}}$  may be quite large. Taking into account the resource limitation of these APs, the potential data rate  $\lambda_\mu$  in Eq. (14) will be very low. So, with high probability all users of this AP will have data rate less the threshold  $\gamma$  in SOA, or will be in the  $\mathcal{C}_R$  in the proposed AWFS algorithm. So, all of these users will assigned to the WiGig access point and leave the LiFi AP unused, which mean underutilization of network resources. Further more, if the threshold  $\gamma$  in SOA algorithm is chosen very low, none or a very small number of users will assigned to the WiGig AP, which is another form of resources underutilization.

In the second proposed CAWFS algorithm, the  $N_{max}$  users are assigned to the WiGig AP one-by-one in consecutive steps. In the beginning, a set  $\mathcal{M}$ , contains all users are constructed and all users are assigned to LiFi APs using Eq. (13). In each step, the user with minimum potential LiFi rate  $\mu_{min}$ , calculated using Eq. (14), is assigned the the WiGig AP, removed from  $\mathcal{M}$ , and the other users, in  $\mathcal{M} = \mathcal{M} - \mu_{min}$ , are redistributed among the LiFi APs using Eq. (13) and the new potential  $\gamma_\mu$  is recalculated. This process is repeated until the number of users, which are assigned WiGig AP, reaches

the maximum allowable number  $N_{max}$ . The APA result of the CAWFS algorithm could be represented as:

$$g_{\mu,\alpha}^{(CAWFS)} = \begin{cases} 1, & \alpha = \begin{cases} \tau_{1,\mu}, & \mu \in \mathcal{M} \\ \text{WiGig AP}, & \mu \notin \mathcal{M} \end{cases} \\ 0, & \text{Otherwise} \end{cases} \quad (20)$$

---

#### Algorithm 3: CAWFS Algorithm

---

**Initialisation:**  $r_{\mu,\alpha}$ ,  $N_{max}$ , the LiFi users set  $\mathcal{M}$  which contains all users and count = 0;

**while** count <  $N_{max}$  **do**

    Calculates  $\tau_{1,\mu}$  and  $\lambda_\mu$ ;

    Assign the user with the minimum data rate,  $\mu_{min}$ , to WiGig AP;

    Update;  $\mathcal{M} = \mathcal{M} - \mu_{min}$ , count = count + 1;

**end**

In RA step, each AP determines the resource portion for its allocated users, according to Eq. (18).

---

## IV. PERFORMANCE EVALUATION

### A. SIMULATION SETUP

In our simulation, the same system setup and simulation parameters given in [13], [17], [19], [22] are used here. Whereas we consider a hybrid network composed of only one WiGig AP and 9 LiFi APs. All LiFi attocells reuse the same frequency band in a circle with 4 m radius under assumption of no optical ICI. The indoor area dimensions are 24 m × 24 m. The distance between each two neighbouring LiFi APs is 8 m. Users are uniformly distributed and moving randomly using the random way point model [38], [39]. With this mobility model, each node selects a target location (i.e., waypoint) to move at a speed selected from a uniformly distributed interval [ $V_{min} = 0.3$  m/sec,  $V_{max} = 0.7$  m/sec]. Once the target is reached, the node pauses for a random time and then selects another target with another speed to move again. Each node continues this behaviour, alternately pausing and moving to a new location, for the duration of the simulation. The other parameters are summarised in Table 1.

In this study, for downlink communications, the comparison between the traditional SOA and the two proposed algorithms is based on measuring of the achievable data rates and the outage probability. The user data rate in state  $n$  for all algorithms is expressed as:

$$R_\mu^{(n)} = \frac{1}{N_\mu} \sum_{\alpha \in \mathcal{C}} g_{\mu,\alpha}^{(n)} k_{\mu,\alpha}^{(n)} r_{\mu,\alpha}^{(n)}, \quad (21)$$

where  $g_{\mu,\alpha}^{(n)}$  is given in Eq. (16), Eq. (19) and Eq. (20) for SOA, AWFS and CAWFS algorithm, respectively.

### B. ACCESS POINT ALLOCATION (APA) TECHNIQUES

In this part, the APA of all algorithms are discussed. In this simulation,  $N_\mu = 15$  mobile users are allocated to 4 LiFi APs and 1 WiGig AP. In AWFS and CAWFS allocation

TABLE 1. Parameters of simulation.

Name of Parameters	Value
<b>LiFi APs parameters</b>	
The LiFi cell radius	4 m
The room height	2.3 m
The conversion of electric to optical power, $\iota$	1
The LiFi AP transmit optical power, $P_t$	10 W
Baseband bandwidth for LED lamp, B	20 MHz
The PD physical area, $A_p$	1 cm <sup>2</sup>
Half-intensity radiation angle, $\theta_{1/2}$	60 deg
Gain of optical filter, $T_s(\theta)$	1.0
Receiver FoV semi-angle, $\Theta_F$	60 deg
Refractive index, $\chi$	1.5
Optical to electric conversion efficiency, $\kappa$	0.53 A/W
Noise power spectral density, $N_0$	10 <sup>-19</sup> A <sup>2</sup> /Hz
The interval for resource allocation, $T_p$	500 ms
<b>WiGig APs parameters</b>	
Number of base station antennas, $N_{BS}$	25
Number of mobile user antennas, $N_{MS}$	9
Maximum number of users for WiGig AP, $N_{max}$	8
Channel SNR,	0 dB
Number of paths, $l$	1

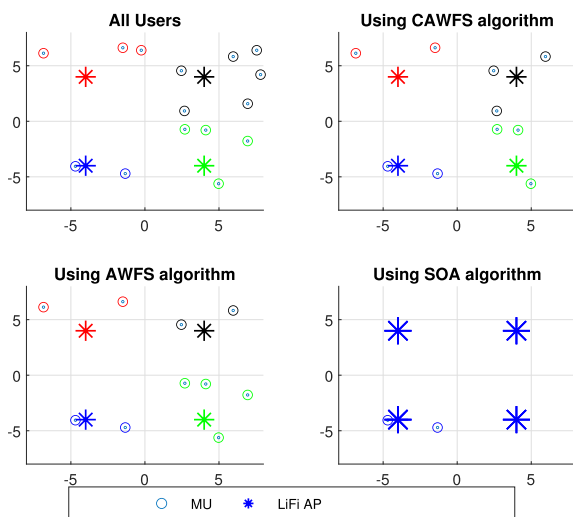


FIGURE 2. APA with high SOA threshold  $\gamma$ .

algorithms,  $N_{max} = 5$ . In Figs. 2 and 3, the APA are shown with SOA threshold  $\gamma$  is very high and very low, respectively. In Fig. 2, for SOA algorithm, 13 mobile users have potential data rates  $\lambda_\mu < \gamma$ , so, they will be allocated to the WiGig AP, and left three out of four LiFi APs unused. In the same time increase the number of users with the WiGig AP, which leads to performance degradation. In Fig. 3, for SOA algorithm, 14 out of 15 mobile users have  $\lambda_\mu > \gamma$ , so, only one user will be allocated to the WiGig AP. In the same time 14 users will be allocated to LiFi APs, which leads to performance degradation too. In the other hand, both AWFS and CAWFS allocation algorithms keep the same number of users in each AP type. Comparing between the AWFS and CAWFS allocation algorithms, it is shown that the CAWFS algorithm

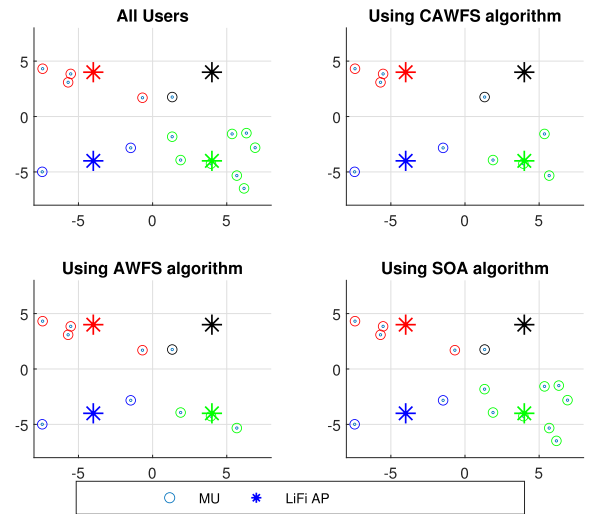


FIGURE 3. APA with low SOA threshold  $\gamma$ .

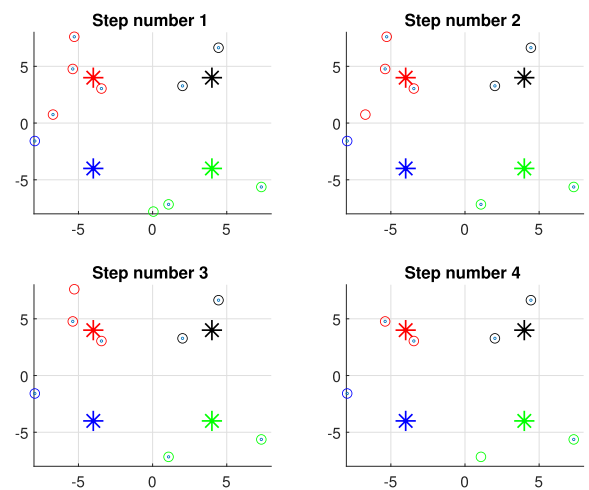


FIGURE 4. Steps in the CAWFS algorithm.

is better because it keeps the different between the number of users allocated to each LiFi AP is as small as possible. Furthermore, in each step, it removes the mobile user with the minimum data rate.

In Fig. 4, using CAWFS algorithm,  $N_\mu = 10$  mobile users are allocated to 4 LiFi APs and 1 WiGig AP  $N_{max} = 5$ . The figure shows the steps of mobile users allocation. In each step, the mobile users with longest distance to its LiFi AP is allocated to WiGig AP.

### C. THE OPTIMAL NUMBER OF WiGig USERS

In IEEE 802.11ad, it is shown that, after a certain number of users, the beamforming performance is inversely proportional with the number of users [9]. In [11], it is proved that with the increasing number of users, the time-elapsd and system complexity are increased, whereas the throughput gain is decreased. In [10], it is proved that with the increasing number of users, beamforming overhead increases linearly,

whereas the throughput gain increases and then decreases. Reference [12] provides a guide to calculate the optimum number of data streams which maximizes the SE. According to [12], the maximum number of spatial degrees of freedom (DoF) is the rank of channel matrix which is equal to  $\min(N_{BS}, N_{MS})$  for the rich scattering channel. Therefore, we only consider the case that  $N_{max}$  does not exceed the  $\min(N_{BS}, N_{MS})$ . In this work, it is assumed that  $N_{BS} = 25$  and  $N_{MS} = 9$ . So,  $N_{max}$  is chosen to be 8 users. In Fig. 5, simulation results show that the maximum number of users could be assigned to WiGig AP  $N_{max} = 8$  users, which agree with the simulation results in [12]. Given that  $\gamma = 10$  Mbps, the outage probability is about 2% and average bit rate is 4000 Mbps per user.

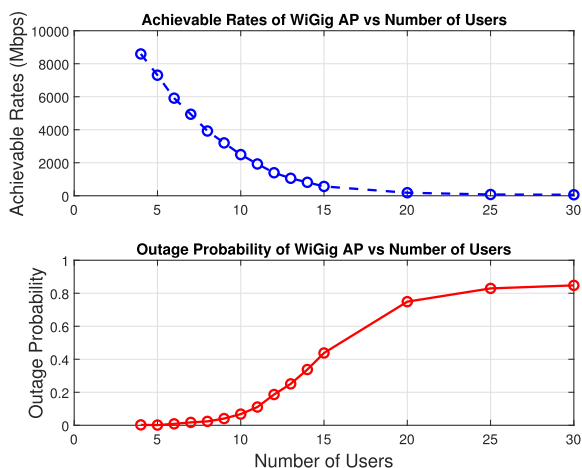


FIGURE 5. Achievable rates and outage probability vs number of users of WiGig AP at  $\gamma = 10$  Mbps.

D. SOA THRESHOLD ( $\gamma$ ) EFFECT

In this part, the maximum QoS and average data rate by all schemes are examined and the effect of the threshold  $\gamma$  in SOA algorithm is evaluated. Fig. 6 shows that the performance of the SOA algorithm is critically dependant on  $\gamma$  value. The best performance of the SOA takes place at  $\gamma_{opt} = 30$  Mbps, this threshold will be used in all coming comparisons.

In the hybrid network, to calculate the outage probability, a unified minimum data rate provided to the users,  $\Gamma_0$ , is considered as the QoS of users. The outage probability of the QoS for each user is:

$$\Phi_0 = \Pr(R_{\mu}^n < \Gamma_0), \tag{22}$$

The outage probability is calculated using Monte Carlo simulations as follows:

$$\Phi_0 = \frac{\sum_n \text{Number of Users with } R_{\mu}^n < \Gamma_0}{\sum_n \text{Number of Total Users}} \tag{23}$$

Fig. 7 shows the outage probability of all algorithms as a function of minimum accepted data rate  $\Gamma_0$ . The simulation results show that the outage probability using the CAWFS

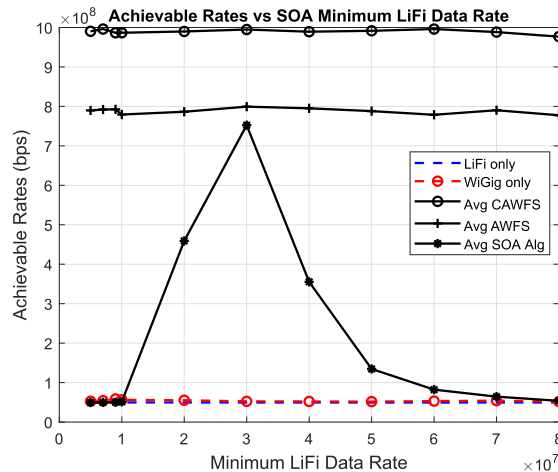


FIGURE 6. Achievable rates vs SOA threshold  $\gamma$  at  $N_{\mu} = 30$ .

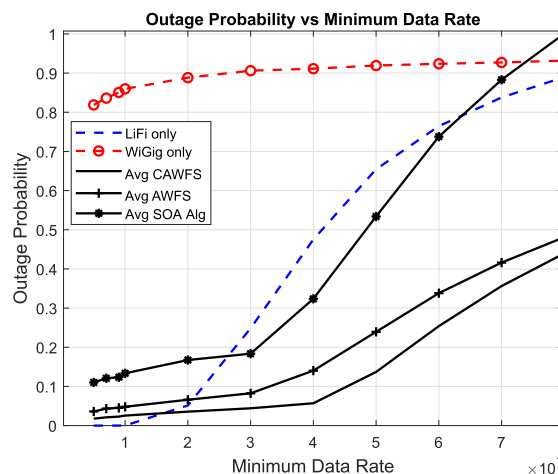


FIGURE 7. Outage probability as a function of minimum accepted data rate  $\Gamma_0$  with  $\gamma_{opt} = 30$  Mbps and  $N_{\mu} = 30$ .

proposed algorithm is less than it in the case of using the AWFS algorithm. Furthermore both are better than the performance in the case of using SOA.

E. NUMBER OF WiGig USERS  $N_{max}$  EFFECT

Simulation results for achievable data rates and outage probability as functions of number of WiGig users  $N_{max}$  are calculated in Figs 8 and 9, respectively. The results show that, for  $N_{max} \leq 8$ , the performance of the CAWFS proposed algorithm is better than the AWFS algorithm. Furthermore both are better than the performance in the case of using SOA.

F. TOTAL NUMBER OF MOBILE USERS  $N_{\mu}$  EFFECT

Simulation results for achievable data rates and outage probability as functions of total number of users  $N_{\mu}$  are calculated in Figs 10 and 11, respectively. The results show that the performance of the CAWFS proposed algorithm is better than the AWFS algorithm. Furthermore both are better than the performance in the case of using SOA.

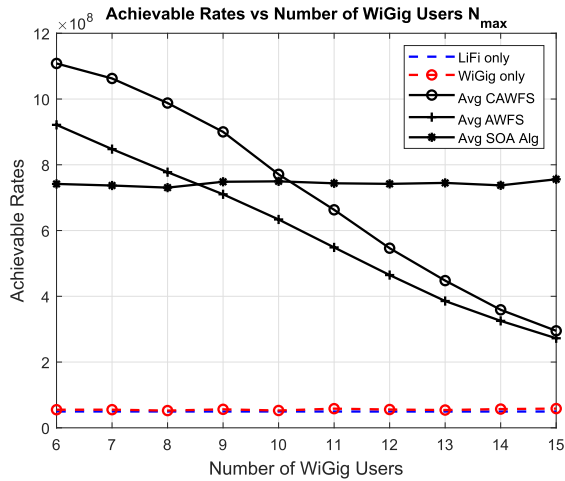


FIGURE 8. Achievable rates vs number of WiGig users  $N_{max}$  at  $N_{\mu} = 30$ .

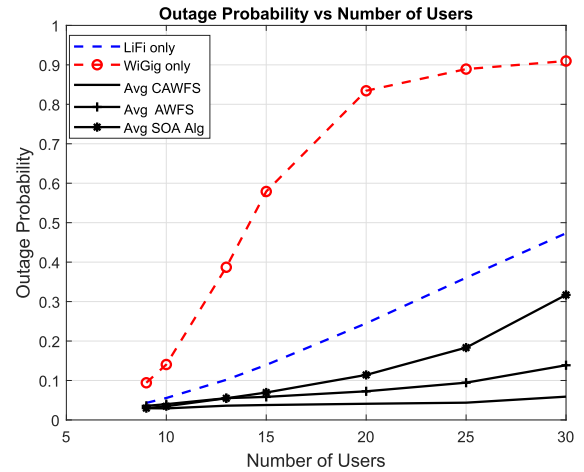


FIGURE 11. Outage Probability vs  $N_{\mu}$ .

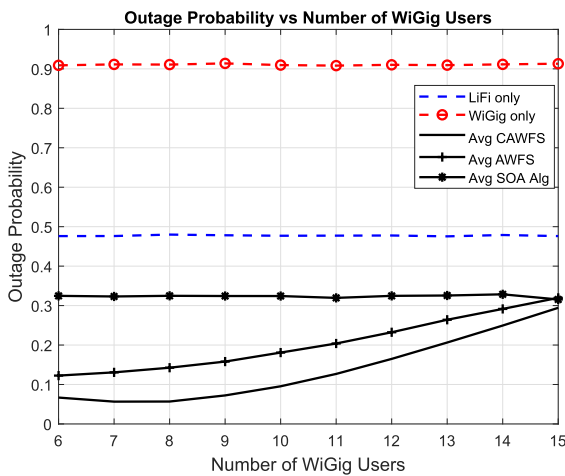


FIGURE 9. Outage Probability vs number of WiGig users  $N_{max}$  at  $N_{\mu} = 30$ .

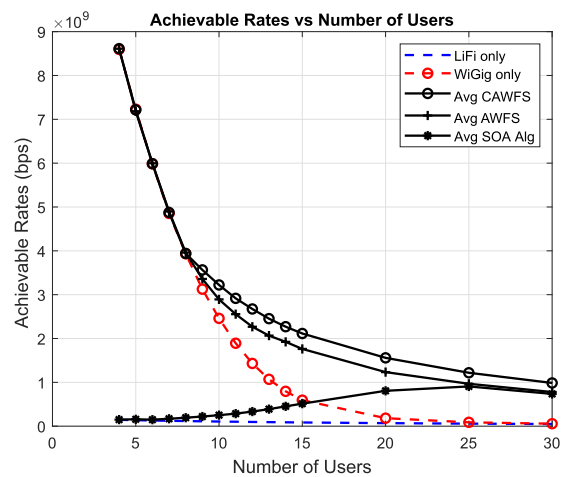


FIGURE 10. Achievable rates vs  $N_{\mu}$ .

Furthermore, according to simulations in Figs 6 to 11, the performance of the hybrid algorithms is better the the performance of the separate LiFi or WiGig algorithm.

### V. CONCLUSION

In this article, Assign WiGig First SOA (AWFS) and Consecutive Assign WiGig First SOA (CAWFS) load balancing schemes in a LiFi/WiGig hybrid network are proposed. In literature, SOA algorithm was introduced to handle this issue. The high degradation in the performance of the WiGig AP with increasing of number of users, more than  $N_{max}$ , motivates to find a modified version of the SOA algorithm. The simulation results show that the performance of the proposed algorithms, measured in the achievable data rates and the outage probability, is completely better than the performance of the SOA algorithm. At the same time, the proposed CAWFS algorithm shows better performance and more complexity when it is compared with the proposed AWFS algorithm.

### REFERENCES

- [1] D. Tsonev, H. Chun, S. Rajbhandari, J. J. D. McKendry, S. Videv, E. Gu, M. Haji, S. Watson, A. E. Kelly, G. Faulkner, M. D. Dawson, H. Haas, and D. O'Brien, "A 3-Gb/s single-LED OFDM-based wireless VLC link using a gallium nitride  $\mu$ LED," *IEEE Photon. Technol. Lett.*, vol. 26, no. 7, pp. 637–640, Apr. 2014.
- [2] H. S. Hussein and M. Hagag, "Optical MIMO-OFDM with fully generalized index-spatial LED modulation," *IEEE Commun. Lett.*, vol. 23, no. 9, pp. 1556–1559, Sep. 2019.
- [3] H. S. Hussein, "Optical polar based MIMO-OFDM with fully generalised index-spatial LED modulation," *IET Commun.*, vol. 14, no. 2, pp. 282–289, Jan. 2020.
- [4] H. S. Hussein, M. Hagag, and M. Farrag, "Extended spatial-index LED modulation for optical MIMO-OFDM wireless communication," *Electronics*, vol. 9, no. 1, p. 168, Jan. 2020.
- [5] M. B. Rahaim, A. M. Vegni, and T. D. C. Little, "A hybrid radio frequency and broadcast visible light communication system," in *Proc. IEEE GLOBECOM Workshops (GC Wkshps)*, Dec. 2011, pp. 792–796.
- [6] D. A. Basnayaka and H. Haas, "Hybrid RF and VLC systems: Improving user data rate performance of VLC systems," in *Proc. IEEE 81st Veh. Technol. Conf. (VTC Spring)*, May 2015, pp. 1–5.
- [7] S. Shao, A. Khreishah, M. B. Rahaim, H. Elgala, M. Ayyash, T. D. C. Little, and J. Wu, "An indoor hybrid WiFi-VLC Internet access system," in *Proc. IEEE 11th Int. Conf. Mobile Ad Hoc Sensor Syst.*, Oct. 2014, pp. 569–574.
- [8] Z. Pi and F. Khan, "An introduction to millimeter-wave mobile broadband systems," *IEEE Commun. Mag.*, vol. 49, no. 6, pp. 101–107, Jun. 2011.
- [9] W. Wu, Q. Shen, M. Wang, and X. Shen, "Performance analysis of IEEE 802.11.ad downlink hybrid beamforming," in *Proc. IEEE Int. Conf. Commun. (ICC)*, May 2017, pp. 1–6.



- [10] I. Ahmed, H. Khammari, A. Shahid, A. Musa, K. S. Kim, E. De Poorter, and I. Moerman, "A survey on hybrid beamforming techniques in 5G: Architecture and system model perspectives," *IEEE Commun. Surveys Tuts.*, vol. 20, no. 4, pp. 3060–3097, 4th Quart., 2018.
- [11] I. Ahmed, H. Khammari, and A. Shahid, "Resource allocation for transmit hybrid beamforming in decoupled millimeter wave multiuser-MIMO downlink," *IEEE Access*, vol. 5, pp. 170–182, 2017.
- [12] G. Kwon, Y. Shim, H. Park, and H. M. Kwon, "Design of millimeter wave hybrid beamforming systems," in *Proc. IEEE 80th Veh. Technol. Conf. (VTC-Fall)*, Sep. 2014, pp. 1–5.
- [13] Y. Wang, D. A. Basnayaka, X. Wu, and H. Haas, "Optimization of load balancing in hybrid LiFi/RF networks," *IEEE Trans. Commun.*, vol. 65, no. 4, pp. 1708–1720, Apr. 2017.
- [14] M. Obeed, A. M. Salhab, and S. A. Zummo, "Joint optimization for power allocation and load balancing for hybrid vlc/rf networks," U.S. Patent 16 163 750, Apr. 23 2020.
- [15] M. Obeed, A. M. Salhab, S. A. Zummo, and M.-S. Alouini, "Joint optimization of power allocation and load balancing for hybrid VLC/RF networks," *J. Opt. Commun. Netw.*, vol. 10, no. 5, pp. 553–562, May 2018.
- [16] A. Adnan-Qidan, M. Morales-Cespedes, and A. G. Armada, "Load balancing in hybrid VLC and RF networks based on blind interference alignment," *IEEE Access*, vol. 8, pp. 72512–72527, 2020.
- [17] Y. Wang, X. Wu, and H. Haas, "Fuzzy logic based dynamic handover scheme for indoor li-fi and RF hybrid network," in *Proc. IEEE Int. Conf. Commun. (ICC)*, May 2016, pp. 1–6.
- [18] Y. Wang, X. Wu, and H. Haas, "Load balancing game with shadowing effect for indoor hybrid LiFi/RF networks," *IEEE Trans. Wireless Commun.*, vol. 16, no. 4, pp. 2366–2378, Apr. 2017.
- [19] X. Wu, M. Safari, and H. Haas, "Three-state fuzzy logic method on resource allocation for small cell networks," in *Proc. IEEE 26th Annu. Int. Symp. Pers., Indoor, Mobile Radio Commun. (PIMRC)*, Aug. 2015, pp. 1168–1172.
- [20] Y. Wang and H. Haas, "A comparison of load balancing techniques for hybrid LiFi/RF networks," in *Proc. 4th ACM Workshop Visible Light Commun. Syst. VLCS*, 2017, pp. 43–47.
- [21] I. Stefan, H. Burchardt, and H. Haas, "Area spectral efficiency performance comparison between VLC and RF femtocell networks," in *Proc. IEEE Int. Conf. Commun. (ICC)*, Jun. 2013, pp. 3825–3829.
- [22] Y. Wang and H. Haas, "Dynamic load balancing with handover in hybrid li-fi and Wi-Fi networks," *J. Lightw. Technol.*, vol. 33, no. 22, pp. 4671–4682, Nov. 15, 2015.
- [23] J. M. Kahn and J. R. Barry, "Wireless infrared communications," *Proc. IEEE*, vol. 85, no. 2, pp. 265–298, Feb. 1997.
- [24] M. Hammouda, S. Akln, A. M. Vegni, H. Haas, and J. Peissig, "Hybrid RF/LC systems under QoS constraints," in *Proc. 25th Int. Conf. Telecommun. (ICT)*, Jun. 2018, pp. 312–318.
- [25] T. Komine and M. Nakagawa, "Fundamental analysis for visible-light communication system using LED lights," *IEEE Trans. Consum. Electron.*, vol. 50, no. 1, pp. 100–107, Feb. 2004.
- [26] C. Chen, S. Videv, D. Tsonev, and H. Haas, "Fractional frequency reuse in DCO-OFDM-Based optical attocell networks," *J. Lightw. Technol.*, vol. 33, no. 19, pp. 3986–4000, Oct. 1, 2015.
- [27] S. Dimitrov and H. Haas, *Principles of LED Light Communications: Towards Networked Li-Fi*. Cambridge, U.K.: Cambridge Univ. Press, 2015.
- [28] A. Alkhateeb, G. Leus, and R. W. Heath, "Limited feedback hybrid precoding for multi-user millimeter wave systems," *IEEE Trans. Wireless Commun.*, vol. 14, no. 11, pp. 6481–6494, Nov. 2015.
- [29] O. E. Ayach, S. Rajagopal, S. Abu-Surra, Z. Pi, and R. W. Heath, "Spatially sparse precoding in millimeter wave MIMO systems," *IEEE Trans. Wireless Commun.*, vol. 13, no. 3, pp. 1499–1513, Mar. 2014.
- [30] A. Alkhateeb, O. E. Ayach, G. Leus, and R. W. Heath, "Channel estimation and hybrid precoding for millimeter wave cellular systems," *IEEE J. Sel. Topics Signal Process.*, vol. 8, no. 5, pp. 831–846, Oct. 2014.
- [31] J. Brady, N. Behdad, and A. M. Sayeed, "Beamspace MIMO for millimeter-wave communications: System architecture, modeling, analysis, and measurements," *IEEE Trans. Antennas Propag.*, vol. 61, no. 7, pp. 3814–3827, Jul. 2013.
- [32] P. Xia, S.-K. Yong, J. Oh, and C. Ngo, "A practical SDMA protocol for 60 GHz millimeter wave communications," in *Proc. 42nd Asilomar Conf. Signals, Syst. Comput.*, Oct. 2008, pp. 2019–2023.
- [33] V. Raghavan and A. M. Sayeed, "Multi-antenna capacity of sparse multipath channels," *IEEE Trans. Inf. Theory*, vol. 1, no. 1, pp. 156–166, Jun. 2008.
- [34] G. J. Foschini, "Layered space-time architecture for wireless communication in a fading environment when using multi-element antennas," *Bell Labs Tech. J.*, vol. 1, no. 2, pp. 41–59, Aug. 2002.
- [35] A. J. Paulraj and C. B. Papadias, "Space-time processing for wireless communications," *IEEE Signal Process. Mag.*, vol. 14, no. 6, pp. 49–83, Nov. 1997.
- [36] A. M. Sayeed, "Deconstructing multiantenna fading channels," *IEEE Trans. Signal Process.*, vol. 50, no. 10, pp. 2563–2579, Oct. 2002.
- [37] J. Mo and J. Walrand, "Fair end-to-end window-based congestion control," *IEEE/ACM Trans. Netw.*, vol. 8, no. 5, pp. 556–567, 2000.
- [38] C.-L. Tsao, Y.-T. Wu, W. Liao, and J.-C. Kuo, "Link duration of the random way point model in mobile ad hoc networks," in *Proc. IEEE Wireless Commun. Netw. Conf. WCNC*, Apr. 2006, pp. 367–371.
- [39] D. B. Johnson and D. A. Maltz, "Dynamic source routing in ad hoc wireless networks," in *Mobile Computing*. Boston, MA, USA: Springer, 1996, pp. 153–181.



**MOHAMMED FARRAG** (Member, IEEE) received the B.Sc. degree in electrical engineering and the M.Sc. degree in communication and electronics from Assiut University, Egypt, in 2001 and 2008, respectively, and the Ph.D. degree in communication and electronics engineering from the Egypt-Japan University of Science and Technology (E-JUST), in 2013. In 2012, he has worked as a Special Researcher Student with Kyushu University, Japan. He has been an Associate Professor with the Faculty of Engineering, Assiut University, since 2019. He is currently working as an Assistant Professor with the College of Engineering, King Khalid University, Saudi Arabia. His research interests include digital signal processing for communications, image denoising, low-power wireless communications, cognitive radio, compressive sensing, Li-Fi technology, and visible light communication. He is also a Technical Committee Member of many international conferences and a Reviewer of many international conferences, journals, and transactions.



**MOHAMMED ZUBAIR SHAMIM** (Senior Member, IEEE) received the M.Eng. degree in electronics and electrical engineering and the Ph.D. degree in electronics engineering and applied physics from the University of Dundee, Dundee, U.K., in 2003 and 2008, respectively. From 2005 to 2009, he has worked as a Research and Development Engineer with Quantum Filament Technologies Ltd., U.K. From 2009 to 2011, he was a Senior Research Scientist with the University of Stuttgart, Germany. From 2009 to 2012, he was the Head of the Department at the Terna Engineering College, University of Mumbai, India. He has been an Associate Professor (micro-nano electronics) with King Khalid University, Saudi Arabia, since 2012. His research interests include fabrication of functional micro-nanostructured surfaces using pulsed excimer laser crystallization and the application of accelerated machine (deep) learning for biomedical and communications applications. He was a recipient of several international awards and scholarships and has published several papers in internationally renowned journals and conferences.



**MOHAMMED USMAN** (Senior Member, IEEE) received the B.E. degree in electronics and communication engineering from Madras University, India, in 2002, and the Master of Science degree in communications, control and digital signal processing and the Ph.D. degree in electronic and electrical engineering from the University of Strathclyde, Glasgow, U.K., in 2003 and 2008, respectively. From 2010 to 2013, he was an Assistant Professor with the Jaypee University of Information Technology, Solan, India. Since 2013, he has been an Assistant Professor with the Department of Electrical Engineering, King Khalid University, Abha, Saudi Arabia. His research interests include mathematical modeling, signal processing, and AI techniques with a focus on wireless communication and biomedical signal processing applications. He is a member of IET. He received the Academic Excellence Award at King Khalid University in 2016. He is also the Organizing Chair/TPC Chair of IEEE International conferences. He serves as a Reviewer for IEEE/Springer/Elsevier journals.



**HANY S. HUSSEIN** (Senior Member, IEEE) received the B.Sc. degree in electrical engineering and the M.Sc. degree in communication and electronics from South Valley University, Egypt, in 2004 and 2009, respectively, and the Ph.D. degree in communication and electronics engineering from the Egypt-Japan University of Science and Technology (E-JUST), in 2013. In 2012, he has worked as a Special Researcher Student with Kyushu University, Japan. He has been an Associate Professor with the Faculty of Engineering, Aswan University, since 2019. He is currently working as an Assistant Professor with the College of Engineering, King Khalid University, Saudi Arabia. His research interests include digital signal processing for communications, multimedia, image, and video coding, low-power wireless communications, one-bit ADC multiple-input multiple-output, underwater communication, index and spatial modulation, Li-Fi technology, and visible light communication. He is a Technical Committee Member of many international conferences and a Reviewer of many international conferences, journals, and transactions. He was the General Co-Chair of IEEE ITCE in 2018.

• • •